Insights into the pion production mechanism and the symmetry energy at high density

中国原子能科学研究院 CHINA INSTITUTE OF ATOMIC ENERGY 中核集团 CNNC

Yangyang Liu, Yongjia Wang, Ying Cui, Cheng-Jun Xia, Zhuxia Li, Yongjing Chen, Qingfeng Li*, Yingxun Zhang*

Phys. Rev. C 103, 014616 (2021).

Abstract: The pion production mechanism is explored based on the ultrarelativistic quantum molecular dynamics model (UrQMD). By analyzing the time evolution of the pion production rate and the central region, we find that characteristic density of pion observable is in the region of 1–2.0 times normal density for Au+Au at E_{beam}=0.4A GeV. The sensitivity of $\pi-/\pi+$ to symmetry energy is weakened after 4–5 *N-Δ-π* loops in the pion production path. The $\pi-/\pi+$ ratio in the reaction near the threshold energies retains its sensitivity to the symmetry energy. By comparing the UrQMD calculations to the FOPI and considering the constraint of symmetry energy from neutron star properties, the slope of symmetry energy L = 54–91.

• Mean field and cross section in the UrQMD*

The isocalar part of potential energy density

$$u = \frac{\alpha}{2}\frac{\rho^2}{\rho_0} + \frac{\beta}{\eta+1}\frac{\rho^{\eta+1}}{\rho_0^{\eta}} + \frac{g_{sur}}{2\rho_0}(\nabla\rho)^2 + \frac{g_{sur,\,iso}}{\rho_0}\left[\nabla(\rho_n-\rho_p)\right]^2 + u_{md}.$$

The momentum dependence interaction:

$$v_{md} = t_4 \ln^2(1 + t_5(\mathbf{p}_1-\mathbf{p}_2)^2)\delta(\mathbf{r}_1-\mathbf{r}_2)$$

The isovector part of potential energy density:

$$u_{sym} = \begin{cases} \left(A\left(\frac{\rho}{\rho_0}\right) + B\left(\frac{\rho}{\rho_0}\right)^{\gamma_s} + C\left(\frac{\rho}{\rho_0}\right)^{5/3}\right)\rho\delta^2 \\ \frac{C_5}{2}\left(\frac{\rho}{\rho_0}\right)^{\gamma_i}\rho\delta^2 \end{cases}$$

α	β	η	g_{sur}	$g_{sur,iso}$	t_4	t_5	K_0	m^*/m
-221	153	1.31	19.5	-11.3	1.57	0.0005	231	0.77

In this work, the Δ–mass dependent *NΔ→ NN* cross sections which were recently calculated based on the one-boson exchange model (OBEM) [1], i.e., $\sigma^{OBEM}_{N\Delta\to NN}(\sqrt{s}, m_\Delta)$, are adopted in the UrQMD model At the given value of m_Δ, it is calculated as

$$\sigma^{OBEM}_{N\Delta\to NN}(\sqrt{s}, m_\Delta) = \frac{1}{1+\delta_{N_1N_2}}\frac{1}{64\pi^2}\int \frac{|\mathbf{p}'_{12}|}{\sqrt{s_{34}}\sqrt{s_{12}}|\mathbf{p}'_{34}(m_\Delta)|} \times \overline{|\mathcal{M}_{N\Delta(m_\Delta)\to NN}|^2}\, d\Omega.$$

In which,

$$\overline{|\mathcal{M}_{N\Delta(m_\Delta)\to NN}|^2} = \frac{(2s_1+1)(2s_2+1)}{(2s_3+1)(2s_4+1)}\overline{|\mathcal{M}(m_\Delta)|^2}.$$

The cross section σ_{OBEM} are shown as red lines in Fig(1).b.

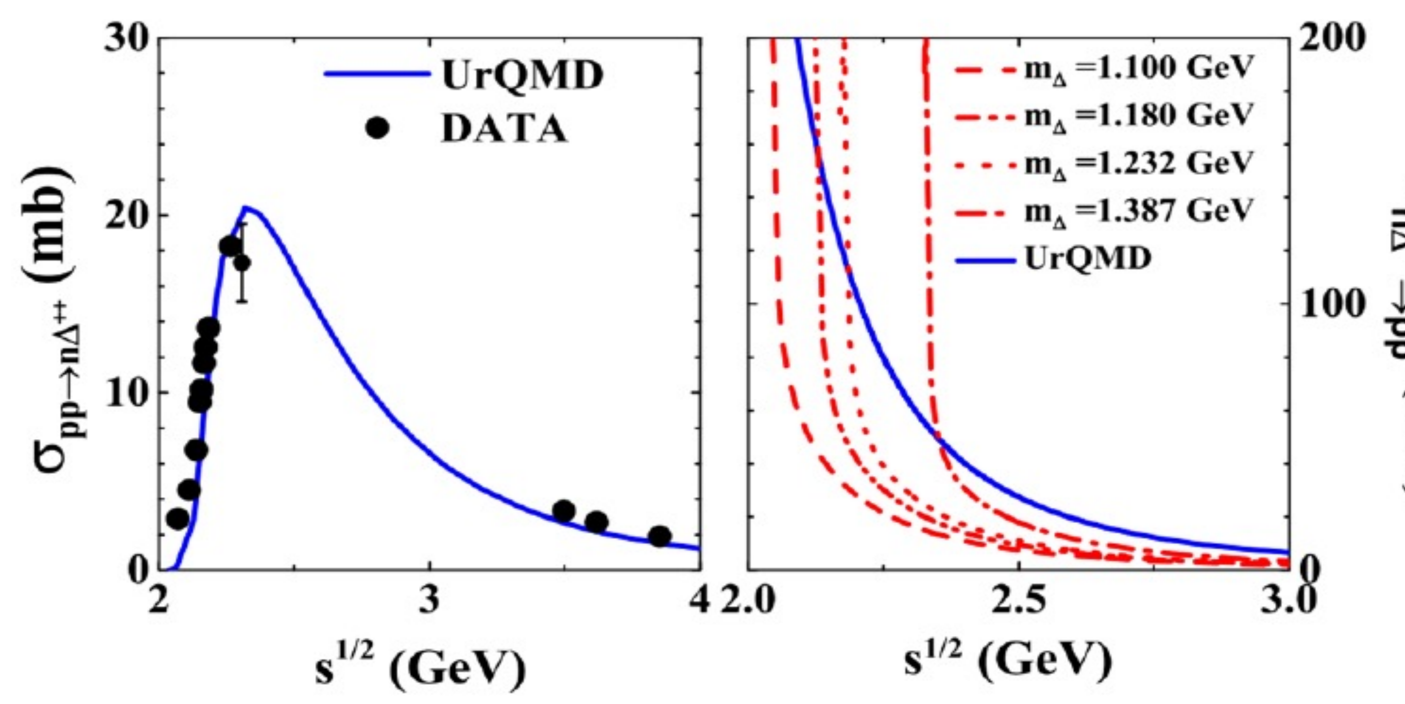

• Pion production mechanism and its characteristic density

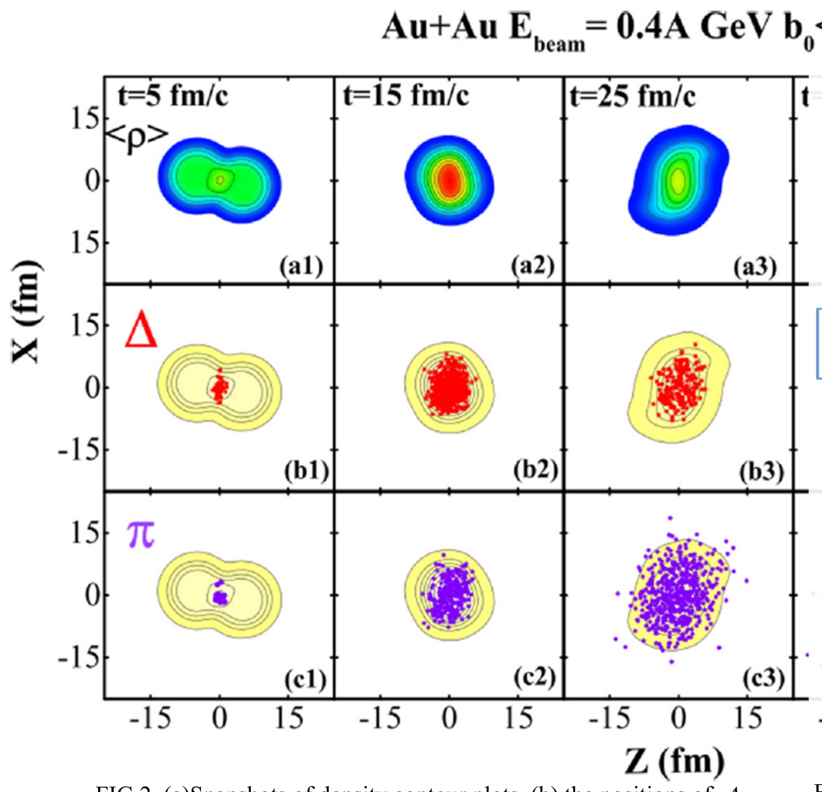

FIG.2. (a)Snapshots of density contour plots, (b) the positions of Δ resonance , and (c) are the positions of π mesons .

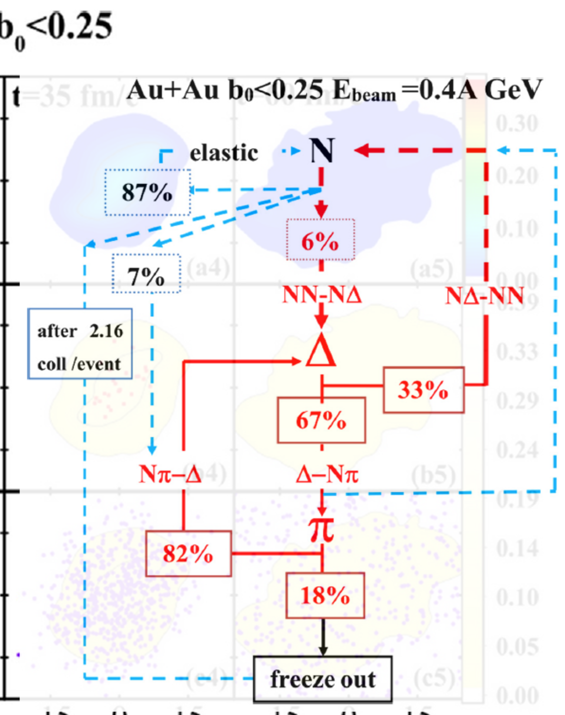

Fig.3. N- Δ -π loops in the UrQMD model, for Au+Au central collision.

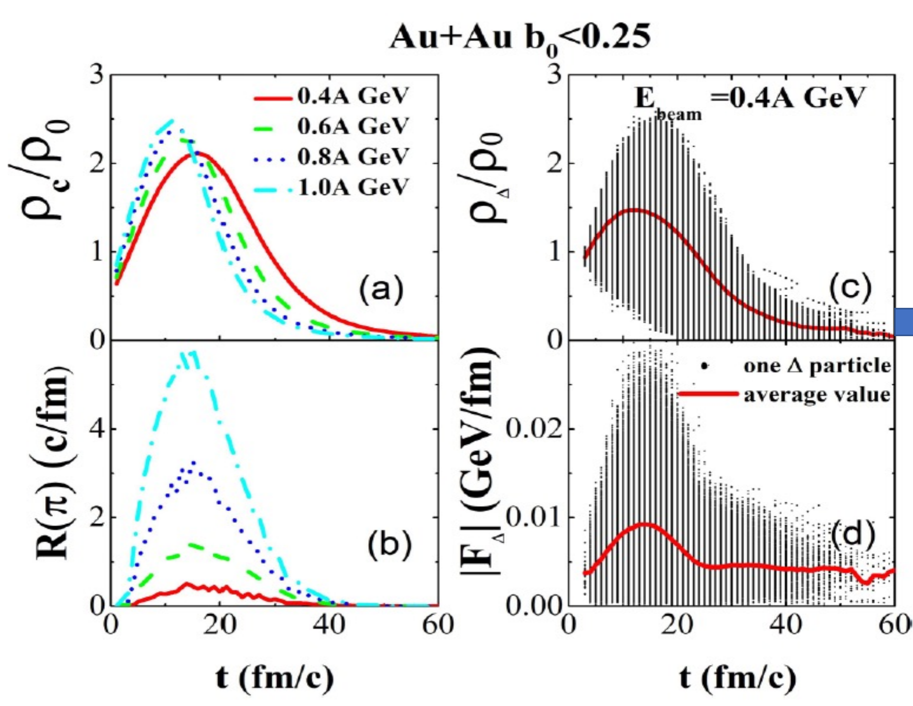

Fig.4.Time evolution of the averaged density (a) and pion production rate (b). Panels (c) and (d) show the density and force of obtained from thousands of events.

$$\langle\rho_c\rangle_\pi = \frac{\int_{t_0}^{t_1} R_\pi(t)\rho_c(t)dt}{\int_{t_0}^{t_1} R_\pi(t)dt} \quad (1)$$

$$\langle\rho\rangle_{F_\Delta} = \frac{\int_{t_0}^{t_1}\sum_i \left|F_\Delta^{(i)}(t)\right|\rho_\Delta^{(i)}(t)dt}{\int_{t_0}^{t_1}\sum_i \left|F_\Delta^{(i)}(t)\right|dt}$$

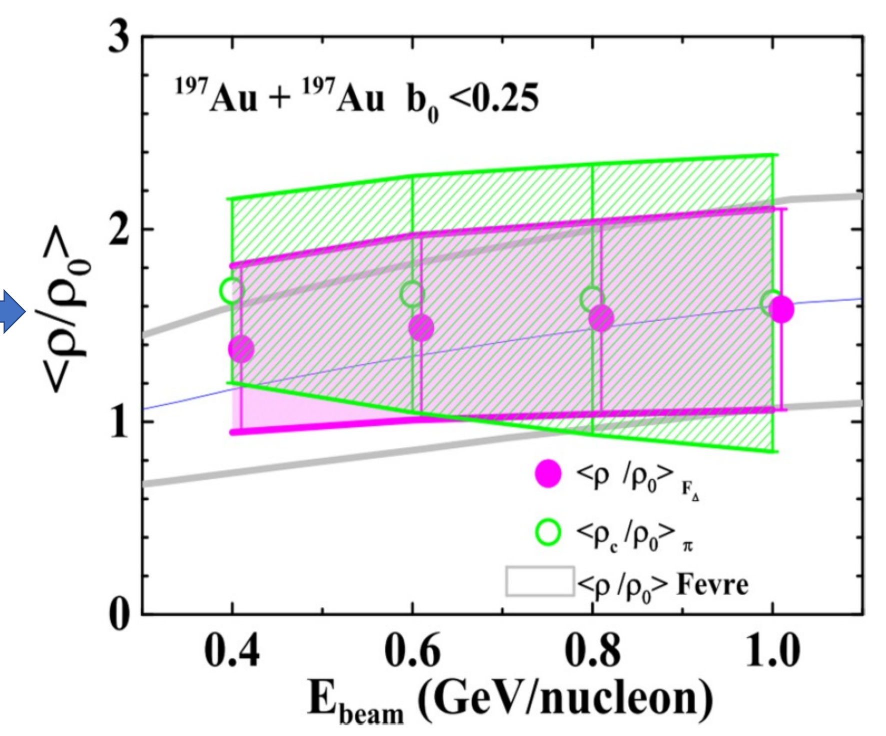

Fig.5 Pion-weighted density and the force acting on Δ weighted density. The region within gray lines is the characteristic density probed by flow observable [2].

The pion freeze out after 4-5 N-Δ–π loops , which will reduce the sensitivity of π–/π+ to the symmetry energy . The characteristic density of pion has been calculated by eq.1, and results show that its characteristic density is in the range of 1–2.0 times normal density at E_{beam}=0.4A GeV .

Effects of $\sigma_{N\Delta\to NN}$, , incompressibility K_0, and symmetry energy on M(π) and π−/π+

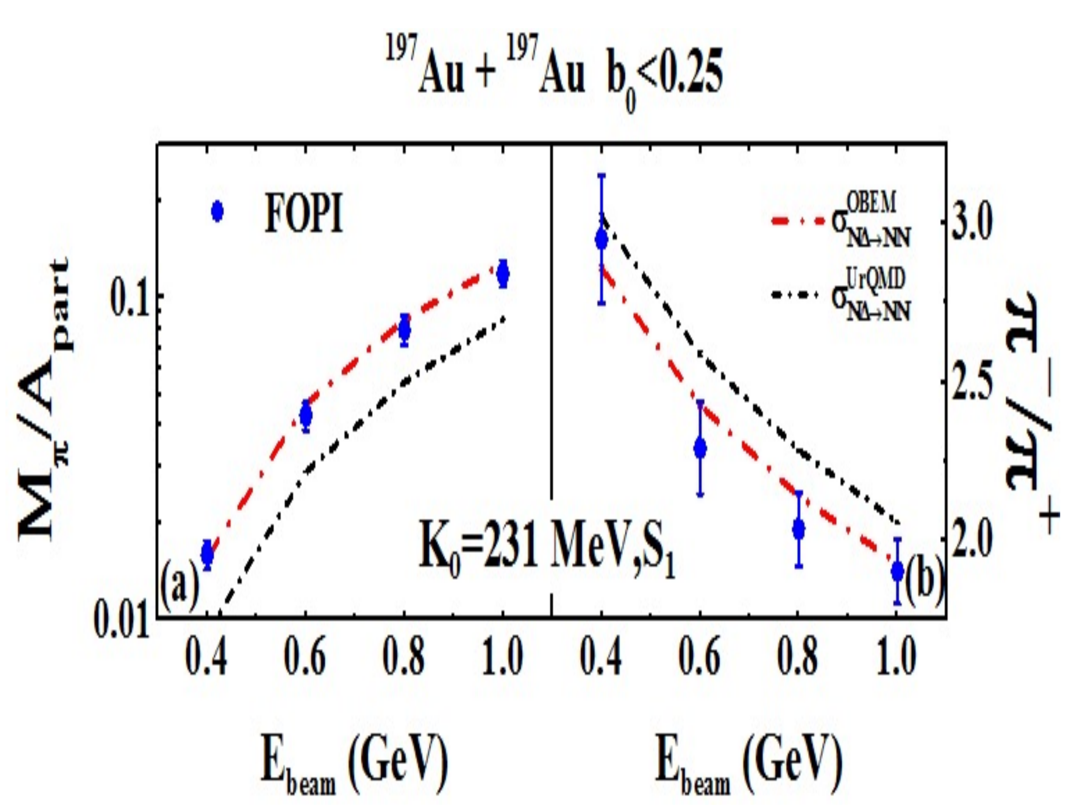

Fig.6. The excitation function of the $M(\pi)/A_{part}$ and $\pi-/\pi+$ with different NΔ-NN cross section.

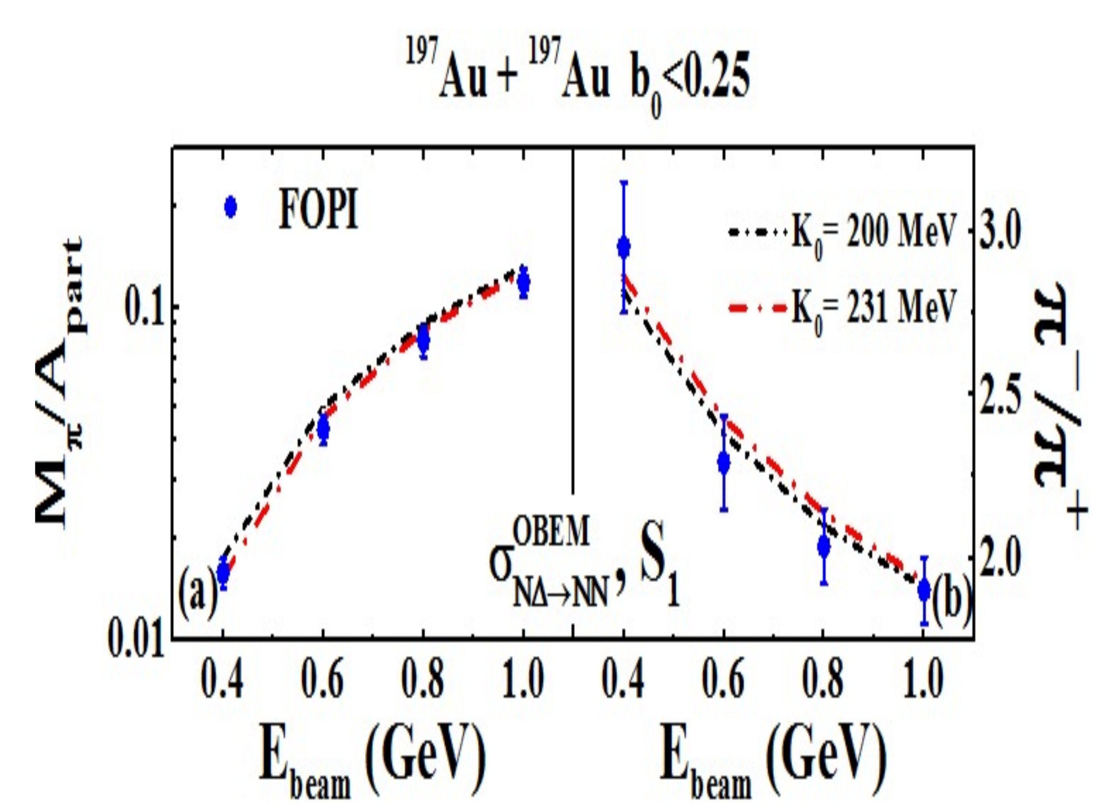

Fig.7. The excitation function of the $M(\pi)/A_{part}$ and $\pi-/\pi+$ with different incompressibility K_0.

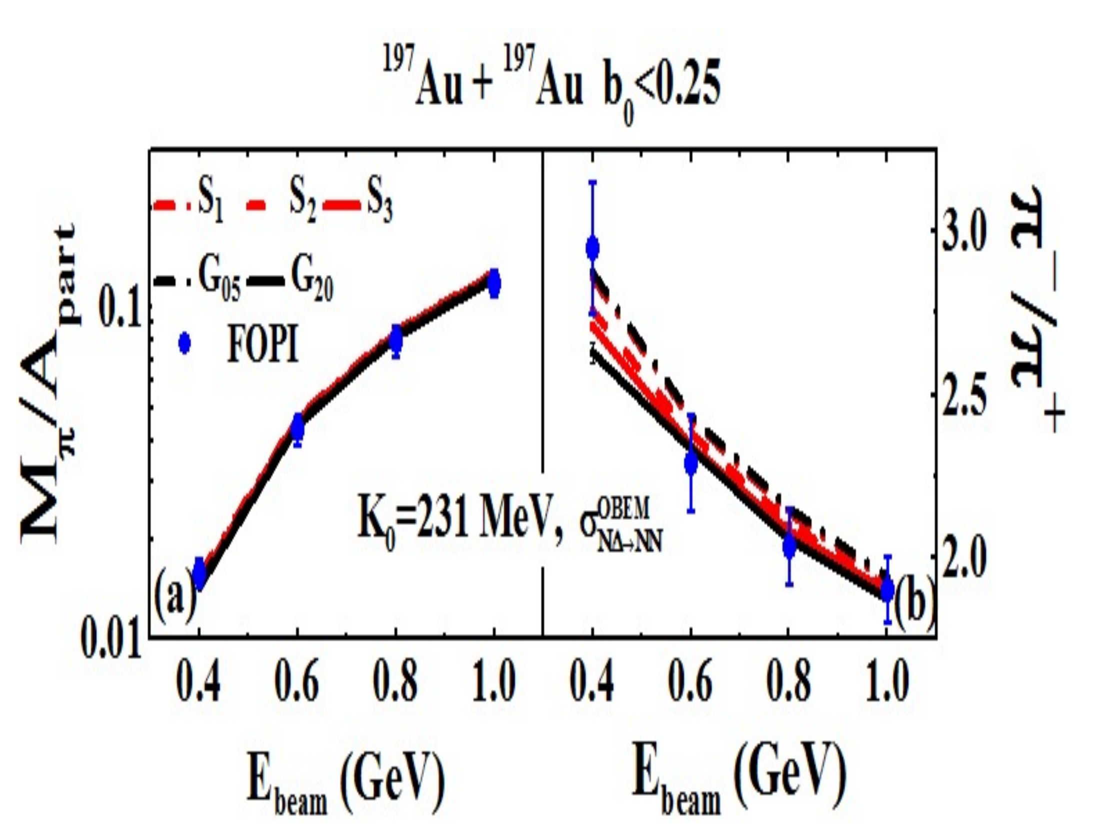

Fig.8. The excitation function of the $M(\pi)/A_{part}$ and $\pi-/\pi+$ with different symmetry energy .

The $\pi-/\pi+$ ratio in the reaction near the threshold energies retains its sensitivity to the symmetry energy, and it is insensitive to the nuclear incompressibility K_0 and effective mass when their values are selected in the commonly accepted range.

Constraints on symmetry energy at high density by $\pi-/\pi+$ and neutron star prosperities.

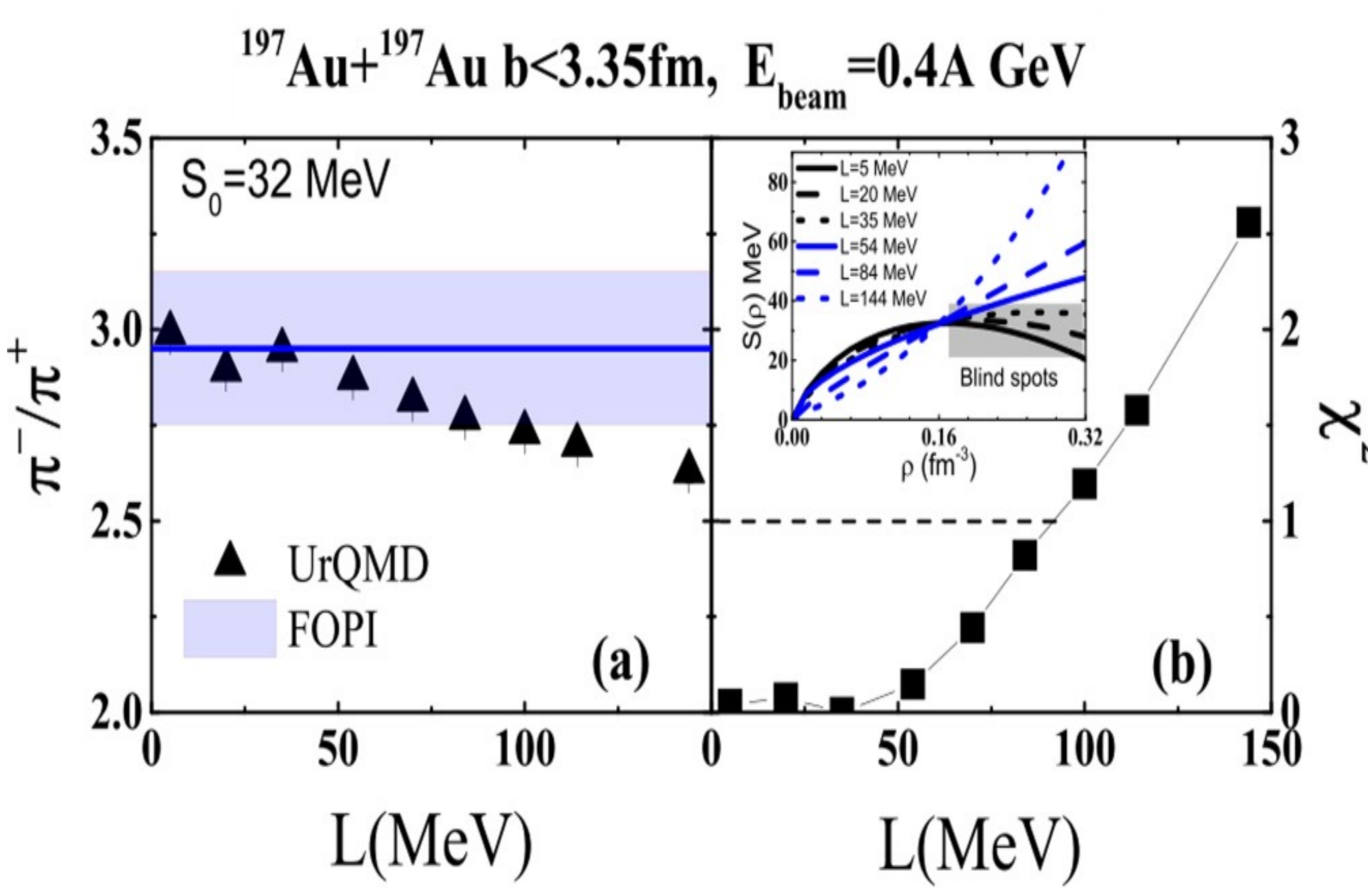

Fig.9. (a) $\pi-/\pi+$, (b) $\chi2$ as a function of L.

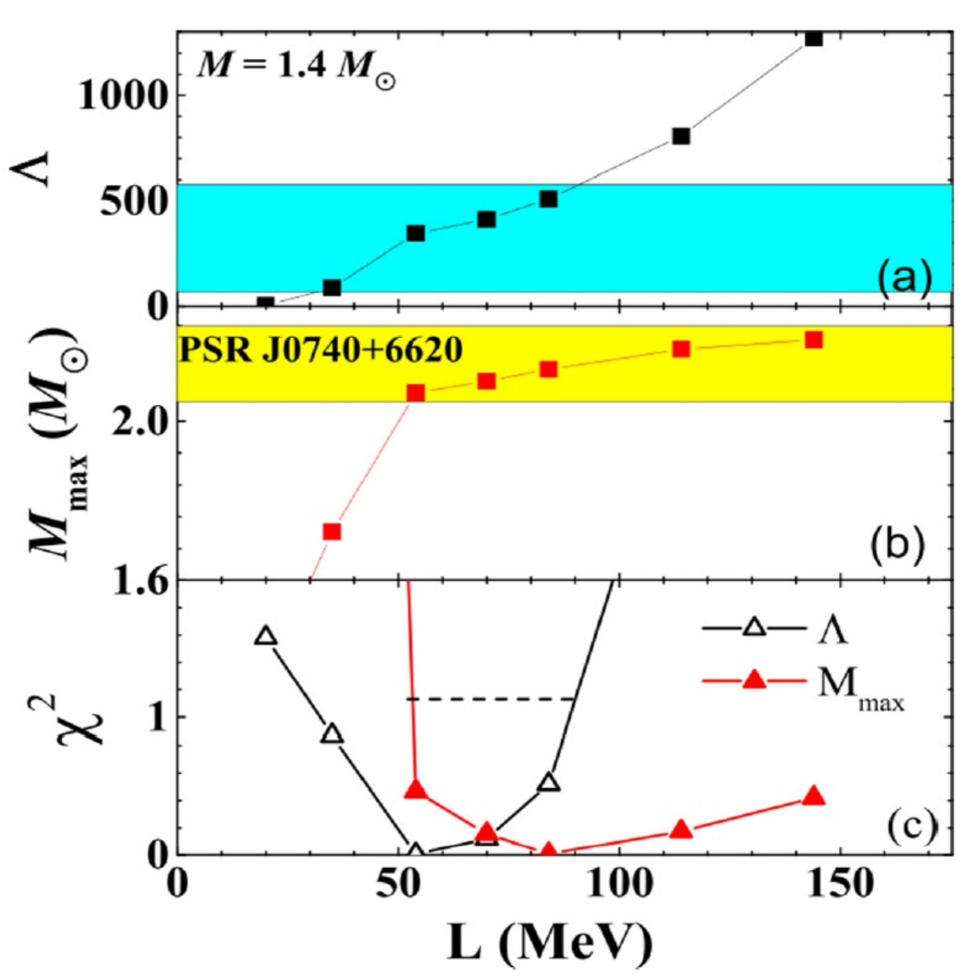

Fig.10.(a)Λ, (b),M_{max} and (c) $\chi2$ as a function of L.

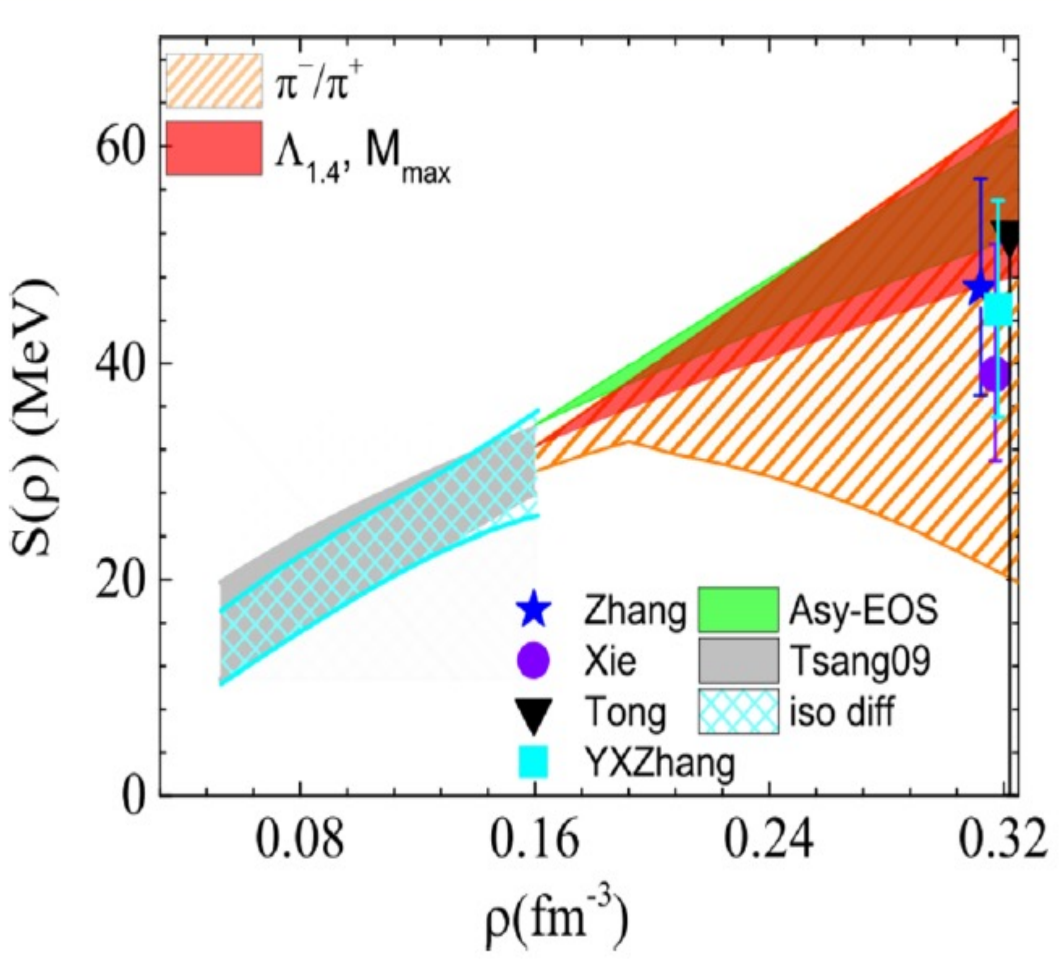

Fig.11.Constraints of density dependence of the symmetry energy.

By comparing the UrQMD calculations to the FOPI data at 0.4*A* GeV and considering the constraint of symmetry energy from neutron star properties, the slope of symmetry energy L = 54–91 MeV and the symmetry energy at two times normal density $S(2\rho_0)$= 48–59 MeV are deduced.